Building a multi-scale surface model of the workspace of a robot manipulator

Yue Liu and Denis Laurendeau

Computer Vision and Digital Systems Laboratory
Department of Electrical Engineering
Laval University, Québec, (Qué), Canada, G1K 7P4
yueliu@gel.ulaval.ca, laurend@gel.ulaval.ca

Abstract

This paper describes a technique for the construction of a multi-scale surface model of the workspace of a robot. The model is based on a triangulation of range data acquired with a random access range finder.

Résumé

Cet article décrit une approche pour la construction d'un modèle de surface de l'espace de travail d'un manipulateur. Le modèle repose sur la construction d'une triangulation de données recueillies à l'aide d'une caméra 3-D à accès aléatoire.

1. Introduction

The goal of computer vision is to allow a machine to understand its environment and perform tasks using perceptual information. The modeling of 3-D scenes is a central problem in the field of computer vision. It is a necessary step in many industrial applications, such as telerobotics and vehicle guidance.

There is a large body of work on 3-D object modeling. The usual approach is to process large volume of information and extract features of objects [1]. Here, we propose a different approach to 3-D workspace modeling. The basic idea is to acquire a minimum amount of 3-D information on the scene, build a coarse model, and then use this model to guide the acquisition of additional data. We call this approach "multi-scale workspace modeling". Two scales are defined: *i)* the Coarse-Scale-Map (CSM) and *ii)* the Fine-Scale-Map (FSM).

The first step is to acquire a CSM of the workspace using a random access range finder and to build a description of the scene using a limited number of points. For this purpose, several sampling strategies have been explored. Since the 3-D data at the CSM contains global, and often sparse, information, the data is organized in a Delaunay triangulation. In the Delaunay triangulation, a large triangle means that the area it covers is relatively unknown when compared to regions of larger triangle density.

The CSM is used to guide the acquisition of additional 3-D data in order to build the FSM. The FSM 3-D data is acquired for different sensor positions that are chosen from a list of candidate viewpoints derived from the CSM. The FSM data is also organized into a Delaunay triangulation that is then used to segment the scene into its constituent parts. The typical scene that was used in this paper contains an electrical insulator mounted on a wooden beam and supporting an electrical line. The goal of the vision system is to build a 3-D surface model of the scene and extract its components to guide a telerobotic maintenance operation, namely the replacement of damaged insulators [7].

The paper is organized as follows. First, the procedure for building the CSM is described as well as the strategy for sampling the 3-D data. Then, the approach that was adopted for the construction of the FSM from the CSM is presented. Finally, the segmentation of the 3-D Delaunay triangulation for finding the location of the beam in the scene is described. Simulation results are presented for each step of the algorithm.

2. Building a coarse planar model of the scene: the Coarse-Scale-Map (CSM)

In robotics, it is often useful to have a coarse description of the workspace. This coarse model can be used to avoid collisions while moving the camera in order to acquire more detailed information on interesting parts of the scene. A coarse model should use a minimum number of points. The sampling strategy of the scene is thus of primary importance. The use of a random access laser range finder seems to be a good alternative to this minimum sampling problem [2]. Such a range finder may access any part of the scene without having to follow a given pattern. It is thus interesting to study different sampling strategies using this type of 3-D sensor.

2.1 The acquisition of 3-D data at a coarse scale using a random access range finder.

Let us say that it is desired to acquire exactly *NUM* 3-D points using a random access range finder. There are several sampling strategies that can be used to acquire this 3-D data.

2.1.1 Random sampling

The most natural acquisition technique is to direct the

range finder at *random locations* on the scene. The results of a typical random sampling experiment are shown in Figure 1. It is easy to realize from this figure that random sampling is not always appropriate since it can ignore some areas of the scene and oversample other areas. It is not insured that the workspace is sampled uniformly.

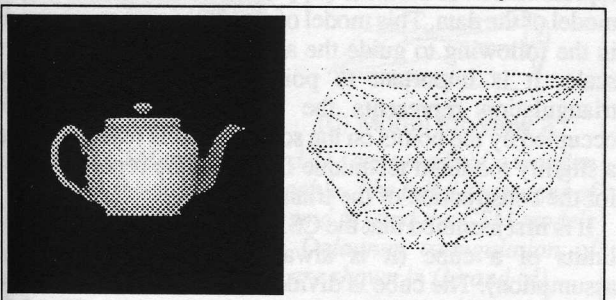

(a) Image of a teapot (b) Random sampling (200 points)

Figure 1 Results of random sampling on the 3-D scene of a teapot. A full 3-D image of the object is shown in (a) while the random sampling of 200 points is shown in (b).The 3-D points in (b) are connected by a Delaunay triangulation

2.1.2 Sinewave sampling

The second approach that was studied is the sinewave sampling technique [8]. Let us assume that the field of view of the image has length L_x along the x-axis and height H_y along the y-axis, and we want to acquire NUM points. We choose the following sinewave sampling function:

$$y = \frac{H_y}{2} \sin \omega x \qquad (1)$$

$$x = \Delta X \cdot K \qquad (2)$$

where ω is the frequency of the sinewave, ΔX is the sampling step and K is the number of points to sample. We can choose ω in advance and adjust ΔX automatically according to NUM. The results of the sinewave sampling of the teapot scene are shown in Figure 2.

Because of its deterministic nature, sinewave sampling allows for a more even coverage of the field of view than random sampling.

2.1.3 Spiral sampling

The scene can be sampled along a spiral curve centered on the optical axis of the sensor. The equation of a spiral curve in polar coordinates is:

$$r = a\theta \qquad (3)$$

When the field of view of the image is $L_x \times L_y$, the equation of the spiral is:

$$a = \frac{L}{2\pi N_f} \qquad (4)$$

where $L = \frac{1}{2} \cdot min\{L_x, L_y\}$. N_f is the circle number of the

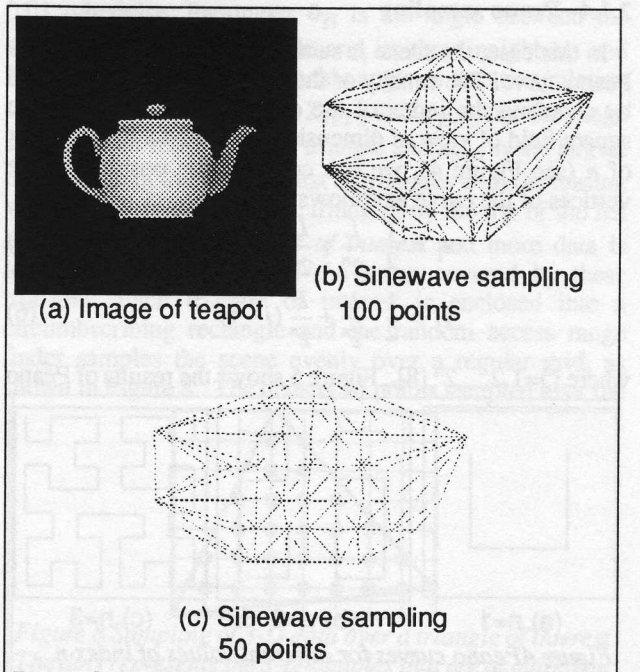

(a) Image of teapot (b) Sinewave sampling 100 points

(c) Sinewave sampling 50 points

Figure 2 Results of the sampling of the 3-D scene of a teapot. A full 3-D image of the object is shown in (a). (b) shows the sinewave sampling of (a) with 100 points and (c) shows the sampling of (a) with 50 points. The 3-D points in (b) and (c) are connected by a Delaunay triangulation.

spiral. So, when the size of the field of view and N_f are given, NUM points can be sampled by adjusting the step angle of the spiral. We can also control the density of points by changing the frequency of the spiral curve [8]. Figure 3 shows the result of spiral sampling on the teapot scene. The

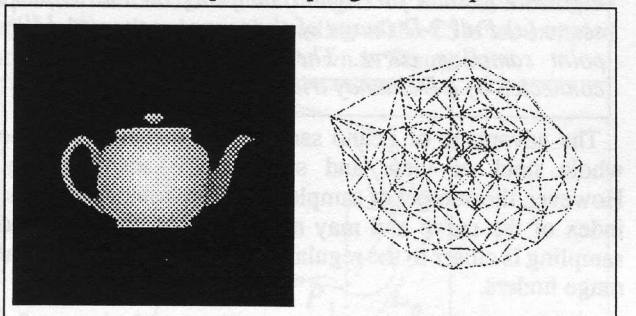

(a) Image of teapot (b) Spiral sampling 100 points

Figure 3 Results of the spiral sampling on the teapot scene. (a) shows a full 3-D image of the object and (b) shows the sampling of 100 points in the scene. Note that the spiral pattern is clearly visible in the Delaunay representation of the data

spiral sampling technique concentrates dada acquisition at the center of the image. This may be interesting when attention must be focused in this area.

2.1.4 Peano sampling

In this case, the scene is sampled along the vertices of a Peano curve. The density of the sampled points is adjusted by choosing the index of the curve [9]. Let us assume a square field of view of dimension $L \times L$ and a Peano index of n (see Figure 4), we can compute the position of the vertices of the curve as follows:

$$x_i = \frac{1}{2} \cdot \frac{L}{2^n} + \frac{L}{2^n}(i-1) \quad (5)$$

$$y_j = \frac{1}{2} \cdot \frac{L}{2^n} + \frac{L}{2^n}(j-1) \quad (6)$$

where i,j=1,2,...,2^n [8].. Figure 5 shows the results of Peano

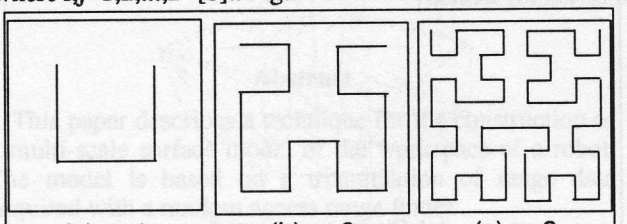

Figure 4Peano curves for different values of index n

sampling on the teapot scene.

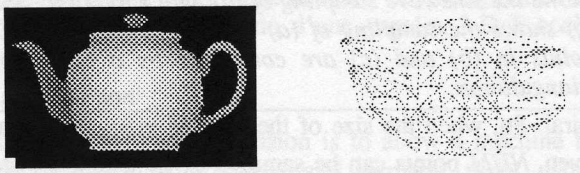

Figure 5 Results for Peano sampling on the teapot scene (a) Full 3-D image of the teapot scene, (b) 149 point sampling curve. The 3-D points in (b) are connected by a Delaunay triangulation.

The advantage of Peano sampling is that it covers the whole field of view and samples the scene evenly. However, the number of sampled points is controlled by the index of the curve and may not be chosen freely. Peano sampling is closer to the regular raster scan of conventional range finders.

2.1.5 Conclusion on the sampling techniques for acquiring CSM data

Each sampling technique presented above has its advantages and weaknesses. For the sampling of the CSM data, we have found that sinewave sampling is the best approach since it allows to *i)* select the number of points, *ii)* change the sampling step and sinewave frequency, *iii)* scan the whole field of view and *iv)* easily implement the sampling strategy.

2.2 Building a Delaunay triangulation as a planar model of the CSM samples

The CSM samples are organized into a connected set using a Delaunay triangulation. The Delaunay triangulation is a well-known approach for the representation of surfaces [3] [4] [6] and provides a planar model of the data. This model of the CSM data will be used in the following to guide the acquisition of data at a finer scale. It is important to point out that the Delaunay triangulation represents the surface, not the volume, occupied by the points on the scene. For this reason, we use a slightly modified technique from the one reported in [6] for the construction of the triangulation.

It is first assumed that the CSM data points fall within the limits of a cube (it is always possible to make this assumption). The cube is divided into tetrahedrons using a standard 3-D Delaunay triangulation technique. The 3-D triangulation is a collection of tetrahedrons which connect sets of four points. Tetrahedrons connected with the limits of the frame of the cube are then eliminated.

Once the 3-D Delaunay triangulation is built, it is desired to keep only the faces of the tetrahedrons that are visible from the camera's viewpoint as a surface model of the scene. This is accomplished by inspecting each tetrahedron of the Delaunay triangulation and deciding when a face is visible from the camera. Two situations may occur as shown in Figure 6. For *type 1)* tetrahedrons, faces *ABD*, *BCD* and *ACD* are kept since they are all visible. For *type 2)* tetrahedrons, only faces *ABD* and *BCD* are kept.

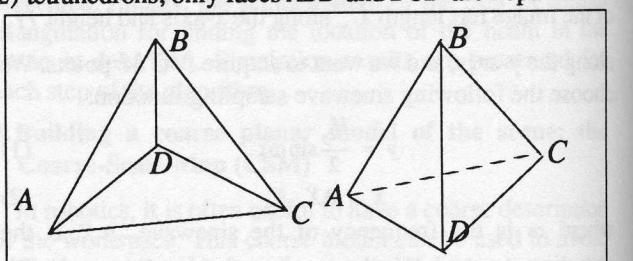

Figure 6 Types of tetrahedrons that may be observed from the camera's point of view

The final surface model contains a list of triangular faces that are visible from the camera's point of view. This provides the CSM model of the scene and is used to guide the acquisition of additional data at the FSM.

2.3 Examples on the construction of the CSM for a complex 3-D scene

The sinewave sampling technique has been used for the acquisition of the CSM data of a complex 3-D scene composed of a wooden beam, an insulator and an electrical wire. Figure 7 shows the resulting CSM models for two different views of the scene.

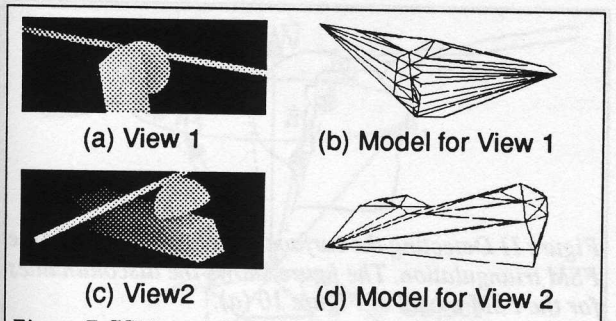

Figure 7 CSM models of a 3-D scene made of a wooden beam, an insulator and a cable. The full 3-D images of the scene are shown in (a) and (c) and the CSM models (i.e. visible faces of the Delaunay triangulation of sinewave sampled points) are shown in (b) and (d)

3. Using the CSM map to acquire more 3-D data. The Fine-Scale-Map (FSM)

The triangulation of the CSM is used to guide the acquisition of additional data in the areas of the scene that look the most *interesting*. The list of triangles of the CSM model is analysed and a figure of merit is computed from the properties of each triangle. The properties that were chosen as significant for the acquisition of the FSM are:

1- the area of each triangle,

2- the maximum angle between the surface normal of a triangle and the surface normal of its three adjacent triangles,

3- the average distance between the centre of mass of a triangle and the camera,

4- vertices of triangles that are the "*most dangerous point*" of the CSM. This "*most dangerous point*" is defined as the point which is the closest to the camera in the CSM. Such a point is clearly visible on the left side of Figure 7 (d).

For each triangle T_i of the triangulation, the figure of merit C_{Ti} is computed from the following equation:

$$c_{Ti} = \frac{1}{w_1 + w_2 + w_3} [w_1 S_{Ti} + w_2 \Theta_{Ti} + w_3 Z_{Ti}] \qquad (7)$$

where:

$$S_{Ti} = f \frac{A_{Ti}}{A_{max}} \qquad (8)$$

$$\Theta_{Ti} = \frac{\theta_{Ti}}{\theta_{max}} \qquad (9)$$

$$Z_{Ti} = \frac{Z_{Ti\text{-}P1} + Z_{Ti\text{-}P2} + Z_{Ti\text{-}P3}}{Z_{max}}. \qquad (10)$$

A_{Ti} is the area of the triangle, and A_{max} is the area of the largest triangle of the CSM. Factor f is set to 1.0 if the triangle is connected to the most dangerous point and set to 0.01 otherwise. Parameter θ_{Ti} is the angle between the surface normal of a triangle and its three neighbors and θ_{max} is the largest value for this angle in the triangulation of the CSM. Finally, $Z_{Ti\text{-}P1}$, $Z_{Ti\text{-}P2}$ and $Z_{Ti\text{-}P3}$ are the range values of the vertices of the triangle and Z_{max} is the largest range value of the CSM. A list of triangles with decreasing values of c_{Ti} is built and the triangles on the top of the list are considered as *triangles of interest* and more data is acquired over the parts of the scene covered by these triangles. Each triangle of interest is enclosed into a circumbscribing rectangle and the random access range finder samples the scene evenly over a regular grid, as shown in Figure 8. The density of points sampled over the triangle may be controlled by changing the sampling step.

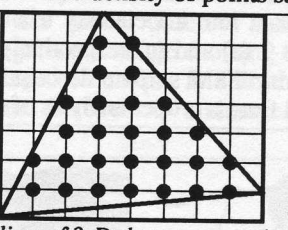

Figure 8 Sampling of 3-D data over a triangle of interest The dots represents the 3-D samples that are acquired on the grid defined by the circumscribing rectangle of a triangle of interest

Aside from triangles of interest that belong to the list built from the CSM, triangles on the outline of the triangulation are also of particular interest. A triangle is said to be on this outline when it is located on its contour. It is important to sample additional data over these triangles in order to get a better knowledge of the contents of the scene. It may happen that a triangle on the outline of the scene is not on the list of triangles of interest mentioned above. The triangles on the outline of the CSM are sampled according to the procedure shown in Figure 9.

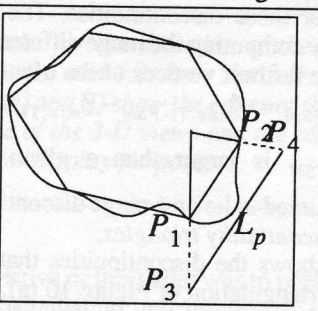

Figure 9 Sampling of triangles located on the outline of the CSM.

We define the area to be sampled as follows: a imaginary line L_p is drawn parallel to the edge P_1-P_2 of a triangle on the contour of the CSM and the points of intersection P_3 and P_4 between this line and the sides of the triangle are computed. The quadrilateral formed by points P_1,P_2,P_3 and P_4 is defined as the area to be sampled around the contour. It is sampled on a regular grid as were the triangles

of interest.

3.1 Structuring the FSM data into a Delaunay triangulation. Result of experiments.

The 3-D data sampled over the triangles of interest and the triangles on the outline of the CSM is called the Fine-Scale-Map (FSM) and is organized into a Delaunay triangulation. Since the data is sampled over a rectangular grid and that the orientation of optical axis of the range finder is the same for all triangles, the triangulation is computed using standard methods [10]. We can think of this triangulation as a "triangulation within a triangulation". Figure 10 (a) and (b) show the results of sampling triangles of interest and outline triangles and organizing the data into a Delaunay triangulation for the scenes in Figure 7 (a) and (c) respectively. It can be seen that a very reliable FSM surface description of the scene may be obtained from a proper analysis of the CSM model.

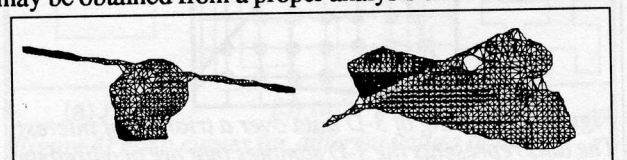

(a) (b)

Figure 10 Results of the sampling of the triangles of interests and of the triangles on the outline of the CSM. (a) shows the result for the CSM of Figure 7 (a) and (b) shows the result for the CSM of Figure 7 (c).The FSM data is organized into a Delaunay triangulation of the 3-D points

3.2 Using the FSM data to get more details near surface discontinuities

Even though the information provided by the FSM is reliable, there may remain uncertainties near surface discontinuities. The FSM triangulation is used to sample more data near those discontinuities. The discontinuities are detected by computing the range difference between the closest and the farthest vertices of the triangle:

$$\partial Z_{Ti\text{-}FSM} = Z_{max,Ti\text{-}FSM} - Z_{min,Ti\text{-}FSM} \qquad (11)$$

When $\partial Z_{Ti\text{-}FSM}$ is larger than a given threshold, the triangle is assumed to lie on a range discontinuity and is put on a list of *discontinuity triangles*.

Figure 11 shows the discontinuities that were detected for the FSM triangulation of Figure 10 (a). We clearly see that the discontinuities between the beam and the insulator are properly detected, as for the discontinuity between the insulator and the electrical wire on top of the insulator.
The areas surrounding the triangles on the list of *discontinuity triangles* are sampled more finely and the data is added to the NTS triangulation. Results are shown in Figure 12.

4. Finding the beam in the scene

The beam is a very important constituent of the scene since it holds both the insulator and the cable. In the following, we show how the FSM triangulation can be used to detect the planes in the scene and then to find which planes belong to the beam.

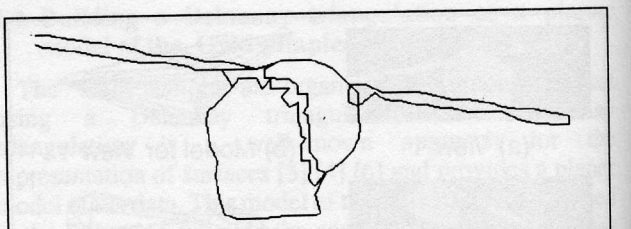

Figure 11 Detecting the surface discontinuities using the FSM triangulation. The figure shows the discontinuities for the FSM model of Figure 10 (a).

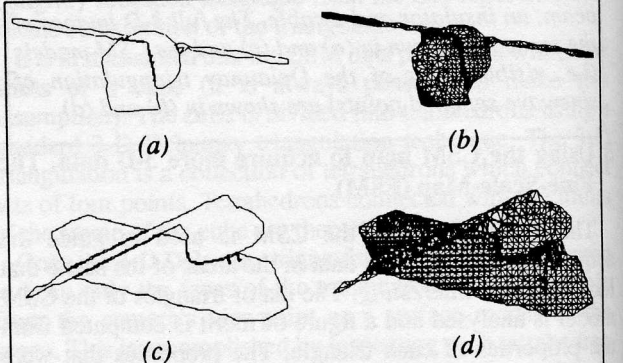

(a) (b) (c) (d)

Figure 12 Result of sampling along discontinuities for three different FSM's . (a) and (c) show the areas that were sampled for the 3-D view of Figure 10 (a) and Figure 10 (b) respectively. (b) and (d) show the final FSM triangulations

4.1 Finding the planes in the FSM triangulation

A very simple yet efficient technique based on Delaunay triangles has been designed to find planar areas of the FSM. The basic idea of the technique is to find the triangles connecting with a given point of the FSM (e.g. which have this point as a vertex) and to compute their unit normal vector. The normal vectors fall within a cone as shown in Figure 13.

The solid angle of this cone can be computed easily and is representative of the curvature of the scene at this point. The curvature is large when the solid angle of the cone is also large. Conversely, a very small solid angle means that the curvature is not important and that the surface is close to a plane. The detection of planes thus consists in finding regions of the scene made of triangles with a small value for the solid angle at each of their vertices. Firstly, the triangles of the FSM having a small value for the solid angle at each of their vertices are found. Each such triangle is thus considered as a seed for a region growing process which merges neighboring triangles with the same surface normal. The growing process is stopped when no triangles can be merged to the region. Figure 14 shows the result of

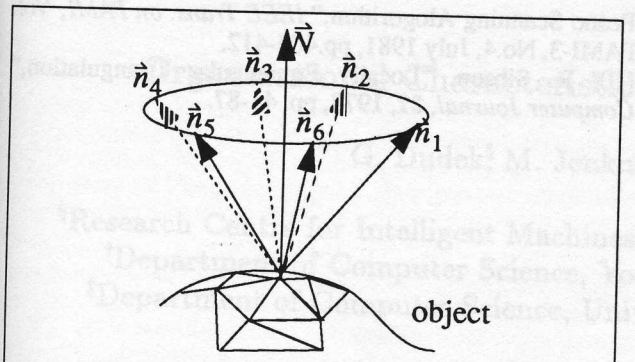

Figure 13 Illustration of the cone formed by the unit normal vectors to triangles having the same CSM point as a vertex

the region growing process for the FSMs of Figure 12 (b) and (d).

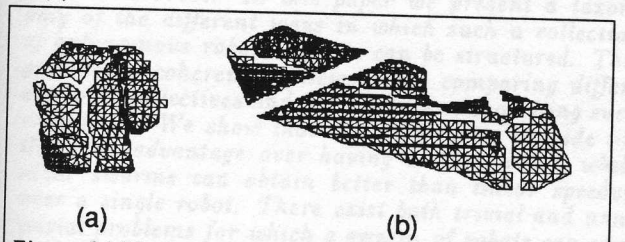

Figure 14 Planar areas found for the FSMs of Figure 12 (b) and (d). In (a), we see that the three visible planes forming the beam are correctly detected. The plane on the bottom of the insulator is also detected. In (b) the planes forming the beam are also detected correctly. The occlusion caused by the cable and the insulator is visible.

4.2 Finding the beam in the set of planes

As shown in Figure 14 (a) and (b), the scene may contain several planar regions which are processed in order to find those that belong to the beam. The first step in this process is to merge planar regions which belong to the same surface but which are separated due to occlusion. Figure 14 (b) is a good example of this phenomenon. The top and left side planes of the beam are occluded by the cable and/or the insulator and are broken into separate parts. The equation of each planar region is computed and those regions which have the same equation are merged. It is assumed that they belong to the same surface.

Once the planar parts have been merged, those parts belonging to the beam are detected using the technique proposed by Fan in [5]. Fan states that when a given plane P_i occludes plane P_j at a jump or a limb, the probability that the two planes belong to the same object is between 0.0 and 0.5. Otherwise, this probability rises between 0.75 and 1.0, that is they belong to same object. By processing each pair of planes, we can divide planes into groups. The group of planes belonging to the beam must be found among these groups.

Several clues may be used to find the beam among the groups of planes. First, the beam is a parallelepiped for which the maximum number of planes that can be seen from a given point of view is limited to three. Furthermore, these planes must intersect one another at right angles.

The pairs of planes are thus processed in order to see whether they satisfy the above constraints.The equation of the line at their intersection in 3-D space is found. This intersection extends to infinity and the endpoints of each line must be found by tracing the lines on each object.

4.3 Results of the detection of the beam in the scene.

The segmentation procedure described above has been implemented and tested on simulated 3-D CSM data and has proven to be very successful in finding the beam. In Figure 15 we see three different CSMs and their corresponding segmented image showing the edges of the beam. The presented technique is able to deal correctly with occlusion and is robust to a change in the point of view.

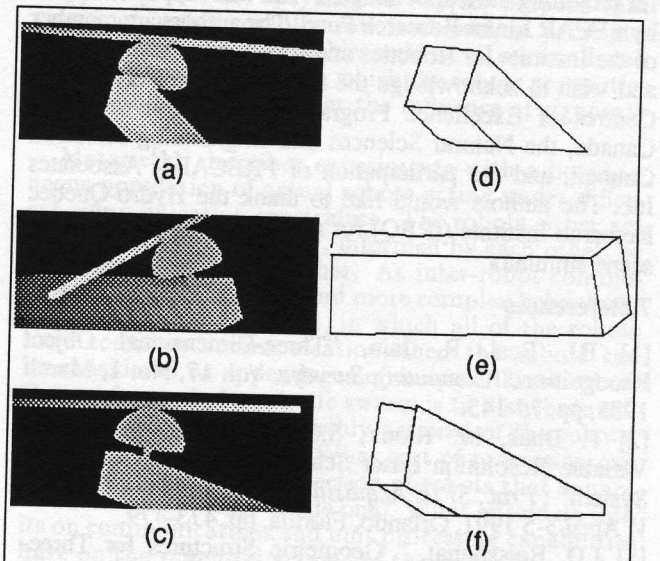

Figure 15 Results for the detection of the beam in the CSM data. (a), (b) and (c) show the 3-D views of the scene and (d), (e) and (f) show the edges of the segmented beam (the scale of the 3-D views and the edge images is not the same) for display purposes.

5. Conclusion

The main objective of this paper was to provide a method for multi-scale acquisition and processing of range data using random access range finding. Two sampling scales were defined. The Coarse-Scale Map contains global information on the scene and organizes this information into a Delaunay triangulation. Several sampling techniques (random, spiral, Peano, sinewave) were studied for the acquisition of CSM data and results were presented for each approach. It was found that sinewave sampling is the one that yields the best results since it provides several control parameters for sampling (frequency, amplitude, sampling step). CSM triangulation of 3-D data is analysed